

# Linear electric field mass analysis: A technique for three-dimensional high mass resolution space plasma composition measurements

DAVID J. MCCOMAS, JANE E. NORDHOLT, SAMUEL J. BAME, BRUCE L. BARRACLOUGH,  
AND JOHN T. GOSLING

Space Plasma Physics Group, Los Alamos National Laboratory, Los Alamos, NM 87545

Communicated by Gian-Carlo Rota, May 10, 1990

**ABSTRACT** A revolutionary type of three-dimensional space plasma composition analyzer has been developed that combines very high-resolution mass composition measurements on a fraction of the incident ions simultaneously with lower mass resolution but high sensitivity measurements of the remaining population in a single compact and robust sensor design. Whereas the lower mass resolution measurements are achieved using conventional energy/charge ( $E/q$ ) and linear time-of-flight analysis, the high mass resolution measurements are made by timing reflected  $E/q$  analyzed ions in a linear electric field (LEF). In a LEF the restoring (reflecting) force that an ion experiences in the direction parallel to the field is proportional to the depth it travels into the LEF region, and its equation of motion in that direction is that of a simple harmonic oscillator. Consequently, an ion's travel time is independent of its initial angle and energy and is simply proportional to the square root of the ion's mass/charge ( $m/q$ ). The measured  $m/q$  resolution,  $(m/q)/\Delta(m/q)$ , for a small LEF-based prototype that we have developed and tested is  $\approx 20$ . In addition, our laboratory measurements with the prototype instrument show that characteristic time-of-flight spectra allow the resolution of atomic and molecular species with nearly identical  $m/q$  values. The measured response of the prototype is in excellent agreement with computer simulations of the device. Advanced design work using this computer simulation indicates that three-dimensional plasma composition analyzers with  $m/q$  resolutions of at least 50 are readily achievable.

Most plasmas observed in space contain a variety of mass species and ionization states in various concentrations. A determination of the distribution of mass and charge states present often allows one to distinguish between different possible sources and sinks for the plasma and can provide information on the sources themselves that is otherwise unobtainable. In addition, measurements of the velocity space signatures of the various ion species present and their evolution in space and time provide essential information on the physical processes affecting the plasmas. Thus considerable effort has been directed toward the development of instrumentation that is capable of resolving different ion species and also suitable for space flight. For planetary magnetospheres, cometary physics, and remote Lunar observations it is desirable to fly extremely sensitive instrumentation with high mass/charge ( $m/q$ ) resolution [ $(m/q)/\Delta(m/q) > 20$  with the exact value depending on the particular application] that is capable of measuring the energy and angular distributions of major and minor constituents over  $4\pi$  sr of space. In this paper we describe a space plasma composition sensor that meets all of these requirements and can be readily optimized for different plasma environments.

The publication costs of this article were defrayed in part by page charge payment. This article must therefore be hereby marked "advertisement" in accordance with 18 U.S.C. §1734 solely to indicate this fact.

Mass spectrometers for measuring space plasma composition have already been developed for numerous spacecraft (1), but unfortunately, to date, these spectrometers have not been able to provide the important combination of (i) nearly complete viewing coverage ( $\approx 4\pi$  sr), (ii) high temporal resolution (a few seconds to tens of seconds) for a mass-resolved set of distribution functions, and (iii) ultra-high  $m/q$  resolution [ $>20 (m/q)/\Delta(m/q)$ ] over a large (tens of kilovolts) energy range. Mass-resolving space plasma sensors for this purpose must have fields-of-view (FOVs) that span at least  $180^\circ$  from the spin axis and have angular resolution of typically  $\approx 20^\circ$  or better in that FOV. As the spacecraft or scan platform spins, such a FOV will sweep out all look directions. In addition, viable space instruments must have very high geometric factors (the product of collection area, energy-angle acceptance, and efficiency) and must be sufficiently compact and low mass to be accommodated within the limited spacecraft resources available (typically  $\approx 10$  kg and  $\approx 10$  W).

In the past, space plasma instruments for mass-resolved plasma measurements have utilized two techniques: linear time-of-flight (TOF) analysis and magnetic mass analysis. Both of these types of sensors require a front end measurement of the incident ion's energy/charge ( $E/q$ ) and post-acceleration of at least the low energy analyzed ions prior to mass analysis. The  $E/q$  measurement is accomplished with some type of electrostatic analysis and additionally provides the energy distributions of the various ion populations. For fast, three-dimensional (3D) measurements of hot magnetospheric plasmas an energy/charge resolution of 10–20% typically is appropriate for the required high sensitivity.

Although much progress has been made over the last several years in the application of magnetic mass spectrometers to space measurements (1–4), such devices have certain inherent drawbacks that limit their applicability for the measurement of hot magnetospheric plasmas. First, magnetospheric plasma analyzers are typically called on to measure ions with energies as high as  $\approx 50$  keV/ $q$ . At these energies, achieving high mass resolution with an instrument that has the necessary very wide acceptance geometry requires a large amount of heavy magnetic material. In addition, the requirement for a large geometric factor (needed to make fast measurements of hot, diffuse magnetospheric plasmas) competes with that for high mass resolution since the aperture size (slit width) needs to be large for the former and small for the latter.

Linear TOF mass spectrometers (1, 5, 6), on the other hand, have the advantage that the entrance aperture to the mass-resolving region can be much larger than in a comparable resolution magnetic mass spectrometer, providing appreciably greater geometric factors for a given size instrument. In this technique an  $E/q$  analyzed ion is postacceler-

Abbreviations: 3D, three-dimensional; LEF, linear electric field; TOF, time-of-flight; FOV, field-of-view; MCP, microchannel plate; FWHM, full width half-maximum.

ated (typically by 10–20 keV/ $q$ ) into a thin foil at the entrance to the TOF section. The start time is defined by the detection of secondary electrons emitted from the back of the foil as the ion passes through. The particle then passes through a nearly field-free TOF region and is detected when it reaches the opposite end of this region, providing a stop time and thus the particle's speed, since the length of the flight path is known.

In a linear TOF device the  $m/q$  of a particle is determined by

$$m/q = 2(E/q) t^2/L^2, \quad [1]$$

where  $L$  is the length of the flight path,  $t$  is the flight time, and  $E/q$  is the sum of the measured  $E/q$  from the electrostatic analysis and the  $E/q$  gained through the postacceleration of the ion. The resolution of the device can then be approximated by taking the absolute value of the first-order terms of the Taylor series

$$\Delta(m/q)/(m/q) = \Delta(E/q)/(E/q) + 2\Delta t/t + 2\Delta L/L. \quad [2]$$

The  $\Delta t/t$  term can be kept small because modern timing techniques, appropriate for space applications, exist that have resolutions of  $<1$  ns and flight times are typically tens to a few hundreds of nanoseconds. Flight path lengths vary because of angular spreading within the foil and the  $E/q$  analyzer and because of finite aperture sizes so that it is difficult to keep the  $\Delta L/L$  term to less than a few percent. However, the most limiting factor for mass resolution is the energy spread of the ions entering the TOF section of the device. This energy spread is caused not just by the resolution of the front end  $E/q$  analyzer but also by energy spreading (straggling) in the thin carbon start foil. Because of the combination of these effects it is very difficult to produce a linear TOF mass spectrometer with  $m/q$  resolution better than  $\approx 5\text{--}7 m/\Delta m$  for reasonable postacceleration voltages.

The magnetic and linear TOF mass analysis techniques suffer from limitations that reduce their utility for making fast, highly mass-resolved measurements of the 3D distributions of hot tenuous plasmas. These intrinsic limitations were the impetus for developing the technique described below, which provides the needed high mass resolution in an instrument capable of making fast 3D measurements.

### Linear Electric Field (LEF) Mass Analysis

Our technique, based on the motion of ions in a LEF region, is an extension of a principle applied to measurements of the solar wind ion composition (7). The basic principle of a LEF plasma analyzer is quite simple. For a  $z$ -directed electric field  $E_z(z)$  that increases linearly with distance along the axis,  $z$ ,

$$E_z(z) = -kz, \quad [3]$$

where  $k$  is a constant solely dependent upon the electromechanical configuration of the device. Since the electrostatic force on a particle is  $qE$ , where  $q$  is the charge of the particle, the equation of motion for the particle in the  $z$  direction is that of a simple harmonic oscillator of mass  $m$ ,

$$m d^2z/dt^2 = -qkz \quad [4]$$

with the solution

$$z = A \sin(\omega t + \phi), \quad [5]$$

where  $\omega^2 = kq/m$  and  $A$  and  $\phi$  are determined by the initial conditions. A particle entering the LEF region at  $z = 0$  will return to the  $z = 0$  plane after having completed half of an oscillation cycle. That is,  $z$  next equals zero when

$$t = \pi/\omega = \pi(m/qk)^{1/2}. \quad [6]$$

Since the bounce time given in this equation is rigorously independent of ion energy and launch direction, extremely high  $m/q$  resolution is possible in a LEF device. The  $m/q$  of a particle is determined from its TOF,  $m/q = kt^2/\pi^2$ . The resolution for such an ideal device is

$$\Delta(m/q)/(m/q) = 2\Delta t/t. \quad [7]$$

That is, it is only limited by the uncertainties in the timing. If a sufficiently linear field is present, very high resolution is possible because the spread in particle energy and angle has no effect on mass resolution. This aspect is particularly important since it is primarily the energy resolution that limits the mass resolution of linear TOF devices.

To the best of our knowledge, the application of a LEF for ultra-high mass resolution measurements in a space sensor was first accepted for the SOHO Mission (7). There, a device was proposed that makes one-dimensional (1D) composition measurements (no angular resolution) of the solar wind beam. A similar 1D LEF-based sensor has also been recommended and accepted for flight on the Advanced Composition Explorer. Measurements from these sensors should provide important new understanding of the solar wind (and hence also solar coronal) composition.

The application of the LEF principle to the measurement of 3D plasma distributions, such as hot magnetospheric populations, is more difficult. In these distributions the various populations must be resolved in  $E/q$  and angle and must be measured over nearly  $4\pi$  sr. Since a spinning spacecraft or scan platform can provide  $360^\circ$  rotation about one axis, an effective fan-shaped FOV of  $180^\circ$  can sample all directions each spin. A  $360^\circ$  FOV is even more desirable and provides two full measurements of all angular distributions twice per spin. In the remainder of this paper we describe a LEF-based sensor that has recently been developed at the Los Alamos National Laboratory to meet all of these design objectives.

### A 3D High Mass Resolution Space Plasma Analyzer

To achieve a  $360^\circ$  FOV, we use a toroidal "top-hat" type of electrostatic analyzer (8) coaxially coupled to a cylindrically symmetric LEF device. Fig. 1 shows a schematic diagram of our sensor. After an ion of appropriate  $E/q$  has been bent through the toroidal analyzer section, it passes through a postacceleration region. The exact voltage used for postacceleration is not crucial, but  $\approx 10\text{--}20$  kV is desirable to accelerate even the lowest energy ions ( $\approx 1$  eV) to energies where they pass efficiently through thin ( $\approx 0.5 \mu\text{g}/\text{cm}^2$ ) carbon foils arrayed around the entrance to the LEF section. It should be noted that though the toroidal top-hat analyzer provides a good means of  $E/q$  analysis for many space plasma environments, it is not the only sort of electrostatic front end that could be mated to a cylindrically symmetric LEF analyzer. Depending on the mission requirements, many other sorts of front ends, such as retarding potential analyzers and/or electrostatic mirrors, could also be coupled to the LEF section. For the special case of a three-axis stabilized spacecraft without a scan platform, nearly  $4\pi$  coverage of space could be obtained by coupling two LEF sections to recently developed  $2\pi$  viewing systems (9), each composed of a toroidal analyzer with a front-end electrostatic deflection system.

Secondary electrons ejected from the backside of the start foil by the passage of the incident particle are used to initiate timing in the LEF region. These electrons are accelerated and focused by the LEF onto a start microchannel plate (MCP) at the opposite end of the device. Their azimuthal location on this MCP gives the azimuthal angle of incidence of the ion

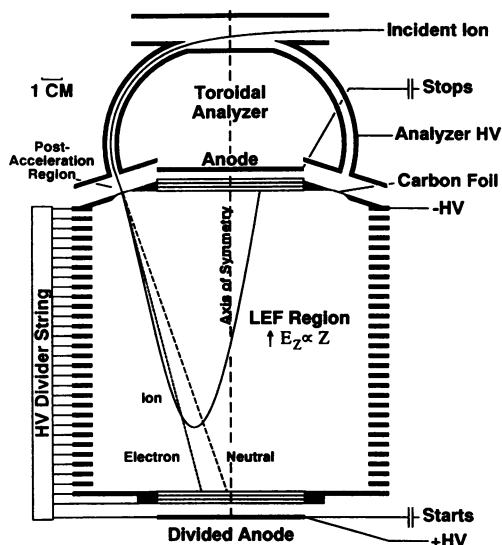


FIG. 1. Schematic diagram of a cylindrically symmetric, LEF-based, 3D space plasma composition analyzer. Incident ions are  $E/q$  analyzed in the toroidal analyzer, postaccelerated, and enter the LEF region through thin carbon foils that eject electrons used to time the start of the particles' flight. If a particle exits the foil ionized, it is reflected in the LEF, providing a high mass resolution measurement (see text). The larger fraction of the particles leaves the foil as neutrals and travels straight through the LEF section. These particles' TOFs provide simultaneous lower mass resolution, but higher sensitivity, composition measurements. HV, high voltage.

(angle around the  $360^\circ$  FOV) at the entrance to the toroidal analyzer.

If the particle exits the foil as a positively charged ion, it is retarded in the LEF and, if the voltage across the device is sufficiently large, the ion is reflected. The reflected ions are detected on a central stop MCP that is in the same plane as the foils and therefore at the same potential. This stops the timing, and the time difference between the ejection of the start electron and this stop pulse provides the ion's TOF.

It is important to note that the foil affects the charge state of the ions; most ion species become predominantly neutral in their transit through the foil. We find that only a small fraction of the incident ions remain positively charged, typically a few to a few tens of percent depending on the species and energy, and are thus suitable for LEF analysis. Independent charge state distribution measurements using somewhat thicker carbon foils show similar results (10).

The consequence of the majority of the particles leaving the foil as neutrals is that only a fraction of the incident ions are analyzed with the high mass resolution LEF technique. However, since the neutrals are unaffected by the electric fields, they pass straight through the LEF region and hit the start MCP at the end of the device, as shown in Fig. 1. These provide ordinary linear TOF measurements by timing between the electron and neutral pulses in the start MCP. Duty cycles are sufficiently low, and TOFs short enough, that there is essentially no confusion between electron starts and neutral stops on the same MCP.

These simultaneous higher sensitivity but lower mass resolution measurements complement the higher mass resolution measurements of the LEF-analyzed ions, significantly increasing the flexibility of the instrument for measuring the many diverse elements of the space plasma environment. In addition, since these neutrals are unaffected by the field within the LEF, they can be used to measure the  $m/q$  of particles that have energies too high to be reflected in the LEF region when they remain charged. This property allows the lower mass resolution, higher sensitivity measurements

to be extended to the upper  $E/q$  limits of the electrostatic analyzer.

A linearly varying electric field within the LEF device is achieved by imposing electrostatic potentials along the boundaries of the LEF region. To provide an electric field that varies linearly with  $z$ , a potential must be applied to the walls of the container that varies as  $z^2$ . As this is difficult to achieve, we have approximated this continuous variation with a series of guard rings (similar to those used in high-energy physics) set at appropriate potentials. These voltages are provided by means of taps along a resistive divider between a negative postacceleration high-voltage power supply (HVPS) and a positive HVPS connected to the start MCP end of the device. Owing to the effects of the constant voltages required on the two ends of the device, the voltages used on the guard rings must increase at a rate that differs somewhat from the theoretical  $V \propto z^2$ . However, with the appropriate choice of voltages, a good approximation to a LEF is achieved, especially away from the edges of the device.

Because a real device does not have a perfectly linear electric field ( $k$  is not quite constant), particles with different initial energies have slightly different TOFs. Although this may appear to be a problem, this effect is quite small for the few tens of percent energy variations introduced by the  $E/q$  analyzer and carbon foil. As the energy variation is relatively small the ion turnaround points are all nearly at the same  $z$  distance within the device (same equipotential line) and thus the effective  $k$  is essentially the same for all of these ions. Deviations from linearity are most pronounced near the entrance end of the instrument but contribute very little to time differences for most particles because the field is small in this region and the ions pass through it quickly. Also, because particles are postaccelerated, there is a minimum energy for most particles entering the LEF region and they must travel deep into the device where the field is quite linear, before reaching a high enough equipotential to cause them to turn around.

### Computer Simulations and Prototype Testing

To examine the applicability of LEF-based sensors for high sensitivity 3D plasma composition measurements, we characterized various sensor configurations through detailed, high-resolution computer simulations. We also verified the LEF concept and the validity of the simulations by comparing the results with laboratory measurements made with a simple prototype device.

A computer simulation package, recently developed at Los Alamos to provide an integrated system for space plasma instrument development, allows different sensor configurations to be analyzed quickly and easily. Once an electrostatic geometry is loaded into the program, a multigrid relaxation routine (11) solves for the potentials (and hence electric fields) throughout the device. Particle trajectories are then traced through the 3D geometry using an improved Euler (12) or Runge-Kutta (13) variable-step-size solver and a four-point field interpolation routine. Once the electrooptics of the device are sufficiently well understood from interactive ray tracing of single particles, a Monte Carlo simulation of the mass resolution is performed over various incident energy, location, and angle passbands.

A number of LEF configurations have been examined with this ray trace code to study the trade-offs between field linearity (and consequently  $m/q$  resolution) and efficiency as a function of such parameters as overall sensor size, height-to-width ratio of LEF region, launch and detection locations, number and layout of guard rings, etc. In all, >50 configurations have been ray traced, yielding a rather detailed understanding of exactly how such devices work. As an

example, the ratio of the LEF region's height (distance along its central axis of symmetry,  $z$ ) to width (distance perpendicular to this axis) strongly affects the resolution and efficiency of these devices. This is because in a cylindrically symmetric, gridless system (no conductors inside the LEF region) there must be a radial electric field acting to push ions out from the central axis wherever there is a linear field retarding their motion in the direction parallel to  $z$ . The consequence is that tall, thin devices, which have more linear electric fields and consequently higher resolution, detect fewer ions on a fixed size central stop MCP and therefore have lower overall counting efficiency. Fortunately, a middle ground can be found in this trade-off (as in many others) that gives good resolution for space plasma composition measurements and a sufficiently high efficiency to be practical for a reasonably sized space sensor.

For testing purposes we developed a small, relatively low-resolution LEF prototype device. Since the optics of the toroidal front end analyzer and postacceleration regions are reasonably well understood, we made only limited tests with such a front end to prove its compatibility with the LEF section. For simplicity, most of the prototype testing was accomplished with the LEF portion of the instrument only.

Fig. 2 compares the Monte Carlo simulation and prototype test results for  $N^+$  and  $O^+$  at 13 keV. The prototype measurements are indicated with the solid line, whereas the ray traced curves are indicated with the dotted line. The energy distribution used for this particular simulation was Gaussian with a 9% full width half-maximum (FWHM). Note the excellent agreement between locations of the two pairs of peaks as well as their approximate widths. The flat noise floor of  $\approx 20$ – $30$  counts per bin is due to random coincidences. This background was measured at count rates of  $1$ – $2 \times 10^4$  Hz and is a strong function of sensor counting rates. It is appreciably lower over much of the range of count rates encountered in space ( $\approx 1$  Hz to  $\approx 5 \times 10^5$  Hz). The elevated tails extending to shorter times are probably caused by slightly shorter bounce times for ions that suffer substantial energy degradation in the thin carbon foil. Nonetheless, the resolution is clearly better than is needed to resolve  $N^+$  and  $O^+$  fully even in this rudimentary LEF device.

In addition to altering charge states and producing energy and angle straggling, the carbon foil also tends to break up molecular ions. Some of the interesting and important ions to be measured by a 3D high-resolution plasma composition

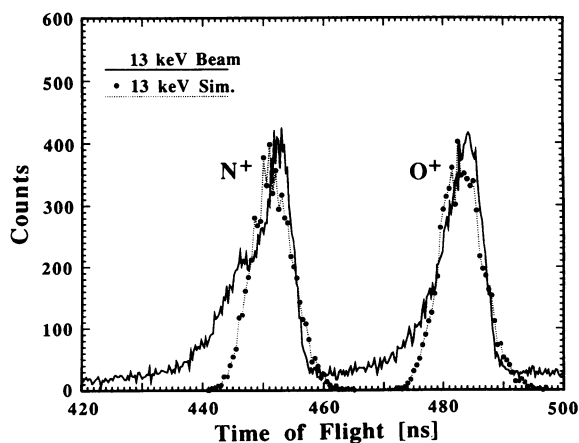


FIG. 2. Comparison of the measured resolution (solid line) of 13-keV  $N^+$  and  $O^+$  in our prototype sensor with a Monte Carlo simulation (Sim.) of this configuration (dotted line). Clearly, the two peaks are well resolved even in such a rudimentary LEF-based sensor. The excellent agreement of the simulation with the laboratory data demonstrates the utility of the simulation for extensions of the design.

analyzer are molecular. A molecular ion passing through the front end  $E/q$  analyzer and postacceleration region arrives at the foil with a nominally known  $E/q$ . Passing through the foil it is usually broken up into fragments that all travel with nearly the same velocity so that the energy is partitioned in proportion to the mass of each piece. These fragments can have appreciably less  $E/q$  than the nominal value and will not travel as deeply into the LEF region of the device as would directly analyzed atomic ions of the same nominal  $E/q$ . Because of the small nonlinearities of a real LEF device, especially at the low-field entrance end of the device, the TOFs of the fragments are slightly shorter than those of the directly analyzed atomic ions, an effect that allows unique identification of molecular ion fragments.

Fig. 3 displays the separation of the  $H^+$  and  $H_2^+$  peaks derived from incident  $H^+$ ,  $H_2^+$ , and  $H_3^+$  in our prototype device. As in Fig. 2, the actual laboratory data are displayed by the solid line and the ray trace simulations are indicated by the dotted line. The two small peaks at longer times are the  $H_2^+$  peaks derived from  $H_2^+$  and  $H_3^+$ . Note that these peaks are much smaller than the  $H^+$  peaks from each of these ions, indicating that nearly all of the molecules incident on the foil break up completely. For  $H_2^+$ , for example, only 1.5% of the incident molecules remain intact in our prototype device's nominal  $0.5 \mu\text{g}/\text{cm}^2$  foil while the remaining 98.5% break up.

The separation observed between the  $H^+$  peaks of various incident species allows for the unambiguous determination of incident species. Such separation is not presently possible with other sorts of space-based mass spectrometers. One example where such separation is important is the case of  $He^{2+}$  and  $H_2^+$ , which have almost identically the same  $m/q$ . This is a particularly important pair of ions to separate because  $He^{2+}$  is a tracer of solar wind ions that penetrate into planetary magnetospheres, whereas  $H_2^+$ , if found inside a planetary magnetosphere, is almost certainly of planetary origin. In a magnetic spectrometer these ions are not separable without a mass resolution of 145 (14) since they have nearly the same  $m/q$ . In our LEF device, however, they are easily separable since (i) most of the  $H_2$  breaks up in the foil and is resolvable from incident  $H^+$  of the same incident  $E/q$  as described above and (ii) most of the  $He^{2+}$  that leaves the foil ionized is  $He^+$  at twice its incident  $E/q$ .

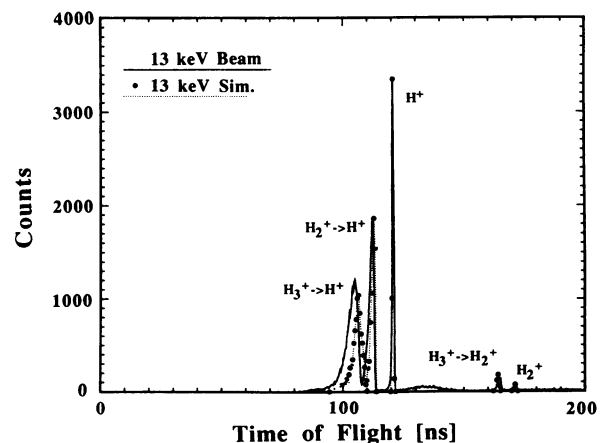


FIG. 3. Measured prototype data (solid line) and computer simulation (Sim., dotted line) of the resolution of the  $H^+$  and  $H_2^+$  components of incident 13-keV  $H^+$ ,  $H_2^+$ , and  $H_3^+$ . Transit through the thin carbon foil breaks up most molecular ions into fragments with energies roughly proportional to their masses. Carefully tailored nonlinearities in the entrance end of the LEF section allow these quite different energy fragments to be resolved and make it possible to provide unique identification of a number of important molecular ions in space.

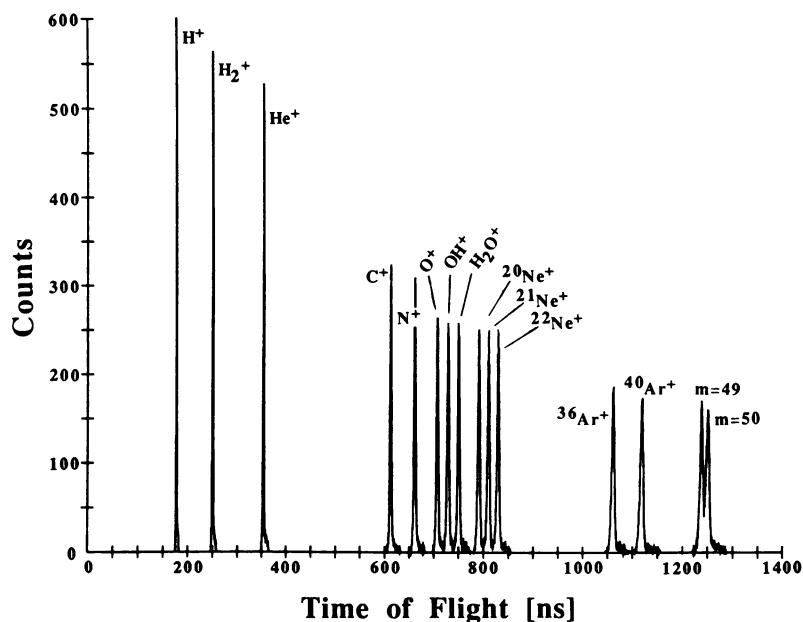


FIG. 4. Monte Carlo simulation of the resolution of an advanced LEF-based sensor. Each of the 13 peaks contains  $\approx 2500$  ion timings taken for an incident 20-keV beam with 10% FWHM energy distribution and varied over sufficient angular range so as to cover fully the stop detector. Note that the neon isotopes and water group ions are fully resolved and that even ions of masses 49 and 50 are resolved at the 25% level.

### Discussion

The excellent agreement between the measured and ray traced results for the prototype LEF described here, along with auxiliary testing of the ray trace code, demonstrates its validity for examining advanced, higher resolution designs. We have examined a number of variations on the basic design in detail.

The computer-simulated mass resolution of one such advanced design that has a good geometric factor and mass resolution is displayed in Fig. 4. For this simulation we assumed incident ion energies of 20 keV with an energy spread of 10% FWHM prior to an additional 20 kV post-acceleration. The maximum incident ion  $E/q$  that can be turned around in this device is  $\approx 25$  keV/ $q$  ( $\approx 45$  keV/ $q$  internal). Note that the isotopic abundances of neon ( $^{20}\text{Ne}$ ,  $^{21}\text{Ne}$ ,  $^{22}\text{Ne}$ ) can be trivially resolved in this device as can the few water group molecules (OH and  $\text{H}_2\text{O}$ ) that remain intact in their transit through the foil. Water group ions (and other molecular ions) can, of course, also be resolved as shifted mass peaks of their atomic components as described above. The mass resolution of this particular design is  $\approx 50$  at the 25% level, as indicated by the peaks for masses 49 and 50. Even greater mass resolution is attainable in a 3D LEF device. We have simulated a number of these higher resolution configurations.

The 3D LEF plasma composition analyzer described here is a revolutionary technique for space plasma mass composition measurements. Its combination of high mass resolution on the positively charged portion of the particles that exit the carbon foil and lower resolution linear TOF measurements of the larger portion that exit as neutrals provides a powerful technique for studying space plasmas. In addition, the ability to provide unique identifications of fragments of molecular ions makes it possible to distinguish between ions that have nearly the same  $m/q$ , such as  $\text{He}^{2+}$  and  $\text{H}_2^+$ .

The 3D LEF composition analyzer described here is a near-ideal candidate for most magnetospheric and planetary missions, and an advanced design similar to that described here has been proposed for the National Aeronautics and Space Administration/European Space Agency (NASA/ESA) mission to Saturn, Cassini. The high resolution and other advantages of this sensor also make it a good candidate for other missions such as NASA's upcoming Lunar Ob-

server. Finally, while this paper has described the uses of a 3D LEF device for space plasma composition measurements, the LEF principle in general, and the cylindrically symmetric version described here in particular, could also have a number of important ground-based applications where a good resolution mass spectrometer is needed within limited mass, power, and volume constraints.

We are grateful to G. Gloeckler for pointing out the general idea of LEF mass analysis to us and gratefully acknowledge valuable discussions with and suggestions by M. F. Thomsen and D. T. Young. Many long hours were spent by J. R. Baldonado, K. McCabe, and N. Olivas, who were instrumental in getting the prototype sensor working in the laboratory. This work was carried out under the auspices of the U.S. Department of Energy.

1. Young, D. T. (1989) *Geophys. Monogr. Ser.* **54**, 143–157.
2. Balsiger, H. (1983) *Adv. Space Res.* **2**, 3–12.
3. Shelley, E. G., Ghielmetti, A., Hertzburg, E., Battel, S. J., Altwegg-von Burg, K. & Balsiger, H. (1985) *IEEE Trans. Geosci. Remote Sensing* **GE-23**, 241–245.
4. Lundin, R., Hultqvist, B., Olsen, S., Pellinen, R., Liede, I., Zakharov, A., Dubinin, E. & Pissarenko, N. (1989) *Geophys. Monogr. Ser.* **54**, 417–424.
5. Wilken, B., Weiss, W., Studemann, W. & Hasebe, N. (1987) *J. Phys. E: Sci. Instrum.* **20**, 778–785.
6. Fritz, T. A., Young, D. T., Feldman, W. C., Bame, S. J. & Cessna, J. R. (1985) in *CRRES/SPACERAD Experiment Description*, eds. Gussenhoven, M. S., Mullen, E. G. & Sagalyn, R. C. (AFGL-TR-85-0017, Air Force Geophysics Lab., Hanscom AFB, MA) pp. 127–139.
7. Hovestadt, D., Geiss, J., Gloeckler, G., Möbius, E. & Bochsler, P. (1988) *ESA SP-1104* (Eur. Space Technol. Center, Noordwijk, Holland).
8. Young, D. T., Bame, S. J., Thomsen, M. F., Martin, R. H., Burch, J. L., Marshall, J. A. & Reinhard, B. (1988) *Rev. Sci. Instrum.* **59**, 743–751.
9. Bame, S. J., Martin, R. H., McComas, D. J., Burch, J. L., Marshall, J. A. & Young, D. T. (1989) *Geophys. Monogr. Ser.* **54**, 441–456.
10. Oetliker, M. (1989) Ph.D. thesis (Univ. of Bern, Bern).
11. Brandt, A. (1977) *Math. Comp.* **31**, 333–390.
12. Boyce, W. E. & DiPrima, R. C. (1986) *Elementary Differential Equations and Boundary Value Problems* (Wiley, New York), pp. 413–417.
13. Press, W. H., Flannery, B. P., Teukolsky, S. A. & Vetterling, W. T. (1988) *Numerical Recipes in C* (Cambridge Univ. Press, Cambridge), pp. 569–580.
14. Neugebauer, M. (1989) *Geophys. Monogr. Ser.* **54**, 389–397.